Diagnosing shaft's damage by engine angular speed fluctuations

D. Boungou[a,b,c] , F. Guillet[a,c], M. El Badaoui[a,c], P. Lyonnet[a,b], R. Toscano[a,b]

September 3, 2012

[a] Université de Lyon, F-42023.
[b] Université de Lyon, LTDS CNRS UMR5513 ECL/ENISE, France.
[c] Université de Saint-Etienne, Jean-Monnet, F-42000,LASPI, F-42334, IUT de Roanne, France.

Abstract

In this paper we study the effect of fatigue from a twisted shaft generating speed fluctuations. Indeed, the speed angular of a rotating machine consists of a DC component (average speed) and fluctuations related to the structure and kinematics of the system. The system studied is a gear train driven in rotation by a direct-current motor. An incremental optical encoder is mounted on the edge of each shaft. We use the square signal generated by this optical encoder to estimate the frequency and instantaneous phase of shafts by the Hilbert Transform. We assume that this phase is a sum of (i) the average phase corresponding to the average velocity, (ii) the phase induced by the system defects, and (iii) the phase induced by mechanical stress which corresponds to the twisted angle of the shaft. The standard-deviation of the instantaneous phase enables us to estimate this twisted angle. Its evolution over time gives us an indiction of the level of shaft damage. So, we propose a new indicator of damage based on the instantaneous phase or the instantaneous frequency.

Key words : Fatigue damage, Hilbert Transform, Instantaneous phase and frequency, Twisted shaft.

1 Introduction

In an engine speed, the shaft misalignment or the mechanical stress, can induce dynamic stresses causing a fatigue damage [SNR-Industry, 2003]. According to this, several studies [D. Shim and Ribbens, 1996], [Desbazeille et al., 2010] [Renaudin et al., 2010] show that shaft speed dispersal reflects the behaviours of mechanical components. Thereby within the framework of a project introduced by the GIPSA-Laboratory of Grenoble, a test bench called GOTIX was conceived. During three years, this bench driven by an asynchronous machine enabled the recording in a synchronous way various signals resulting from several sensors, for example accelerometers,tension sensors, speed and temperature sensors, and optical encoders on which we will base our further study. So after 700 hours, the input shaft was broken and we observed an increase of the standard-deviation of speed until breakage.

This paper is organised as follows : in the first part, after the description of the test bench, we make a spectral analysis of the optical encoder's signal. In the second part, after a description of the twist of a rotating shaft, we propose an instantaneous phase model. Subsequently, in the third part, using the square wave given by an optical encoder, we estimate the instantaneous phase $\theta_i(t)$ with the Hilbert Transform. Fourthly, under some assumptions, considering the suggested model, we try and find a relation between the standard-deviation of the instantaneous phase and the twisted angle. Finally, this trend is used as fatigue damage indicator. A damage model proposed by Lemaitre and Chaboche is used to explain this trend and quantify the damage scalar D.

2 Diagnosis of the test bench GOTIX

2.1 Description of test bench

The test bench GOTIX figure(1)(a) is driven by a three-phase induction-drive motor Leroy Somer 55 kW, slowed by a direct-current motor. It is either powered by 50 Hz or by an adjustable speed drive from 0 to 900 rev/min. The mechanical system is a gearbox multiplier with a speed ratio of 57/15. The bench is equipped with several sensors : 8 accelerometers, 3 hook-on ammeters , 3 potential difference sensors, a torquemeter with speed measurement, speed sensors, 2 optical encoders, 4 temperature sensors. The signal acquisition is done on 20 parallel channels synchronously sampled at 25kHz during 80 seconds (except in special cases). Racal and Oros systems are used. Electrical and mechanical measures are all synchronous, which is one of originalities of the GOTIX test bench.The bench has worked three years, during which, after 700 hours , we observed the breaking of the input shaft figure(1)(c), and an increase in the standard deviation of the speed signal. In the following we propose an explanation for this trend.

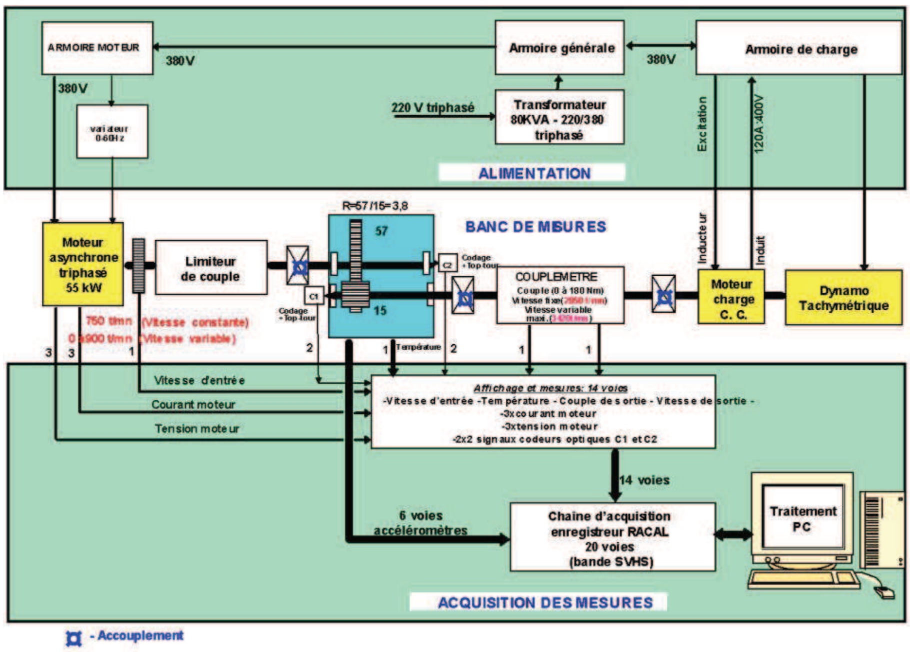

(a) System data acquisition

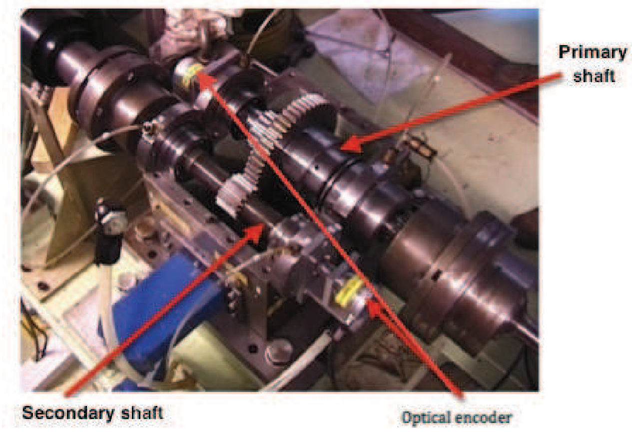

(b) Mechanical system

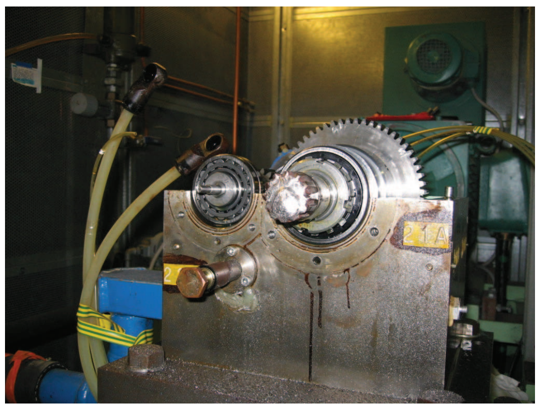

(c) broken

Figure 1: BOTIX test bench

2.2 Technical information about the test bench

Kinematics of the test bench :

- **Motor** : three-phase induction-drive motor Leroy Somer 55 kW.
- **Speed Ratio**: R : 3,8
- **Input shaft** : frequency : 12.3Hz, diameter : 145.5mm, 57 teeths , material : 30CND8, rotational guidance : bearings 20208 TN9 and NU206 ECP.

- **Jack shaft** : frequency : 46.74Hz,, diameter : 45.5mm, 57 teeths , material :17CND6, rotational guidance : bearings 22206.
- **Gear mesh frequency**: 701.1 Hz.
- **Torque**: 145Nm.
- **Sample frequency** : 100KHz.

2.3 Spectral analysis of the optical encoder's signal

Let $x(t)$ the optical encoder's square wave which contains information about the mechanical system (kinematic, mechanical stress,...). These information appear under the form of a frequency modulation which expression is

$$x(t) = A_c \sum_{n=0}^{\infty} \frac{sin\Big[(2n+1)(2\pi f_p.t + \sum_i^k \Phi_i(t))\Big]}{2n+1}, \tag{1}$$

with :
- A_c the modulated signal amplitude,
- f_p the carrier frequency,
- $\sum_i^k \Phi_i(t)$ the modulated signal phase,
- n an integer.

Let $m_i(t)$ the harmonics signals modulating in frequency $x(t)$ with f_i their frequencies and A_i their amplitudes. In this case, the deviation of the instantaneous frequency of $x(t)$ is proportional to $m_i(t)$; $\frac{d\Phi_i(t)}{dt} = \alpha_i m_i(t)$. This implies that :

$$f_m(t) = f_p + \frac{1}{2\pi}\sum_i^k \frac{d\Phi_i(t)}{dt} = f_p + \frac{1}{2\pi}\sum_i^k \alpha_i m_i(t) \tag{2}$$

where :
- $f_m(t)$ is the instantaneous frequency of the modulated signal $x(t)$,
- k is a positive integer corresponding of the number modulating signals .

So we can write Eq(1) as follows :

$$x(t) = A_c \sum_{n=0}^{\infty} \frac{sin\Big[(2n+1)(2\pi f_p.t + 2\pi \sum_i^k \alpha_i m_i(t))\Big]}{2n+1} \tag{3}$$

Based on the Bessel functions, we can decompose $x(t)$ in Fourier series and note that its spectrum includes the frequencies f_p(carrier), and $\delta_{f_i}(f_p)$ which are the harmonics to the right and left of the carrier as shown in the figure 2(a)

$$\delta_{f_i}(f_p) = A_c \sum_{m=-\infty}^{\infty} J_m(\beta_i)\delta(f_p \pm m.f_i), \tag{4}$$

with :
- $J_m(.)$ the Bessel coefficients,
- β_i the modulation index which expression is $\beta_i = \frac{A_i.\alpha_i}{f_i.2\pi}$.

If the set $\Big\{f_i\Big\}_{i=1}^{\infty}$ are the system's caracteristics frequencies namely :

- $f_1 = 700Hz$ the gear mesh frequency,
- $f_2 = 12,3Hz$ the input shaft frequency,
- $f_3 = 46,7Hz$ the jack shaft frequency...

by spectral analysis of $x(t)$ we can find all the above frequencies, as illustrated in figure 2(b) and 2(c).

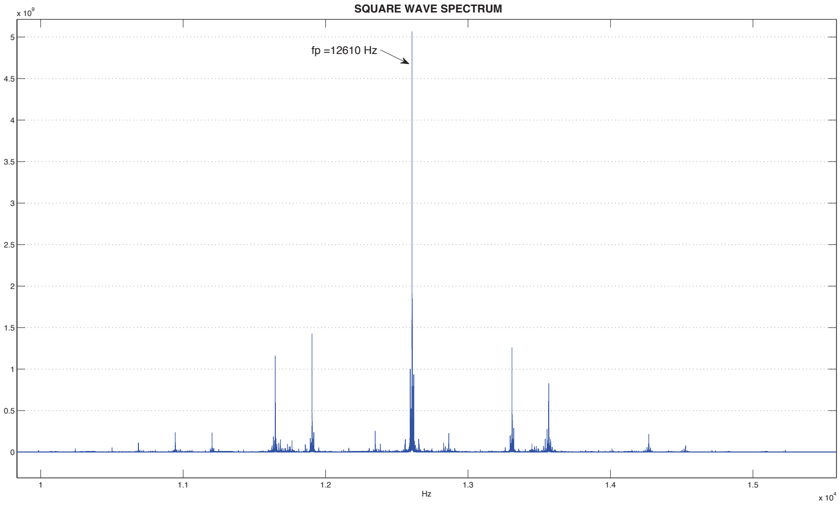

(a) Frequency modulation $f_p \pm m.f_i$

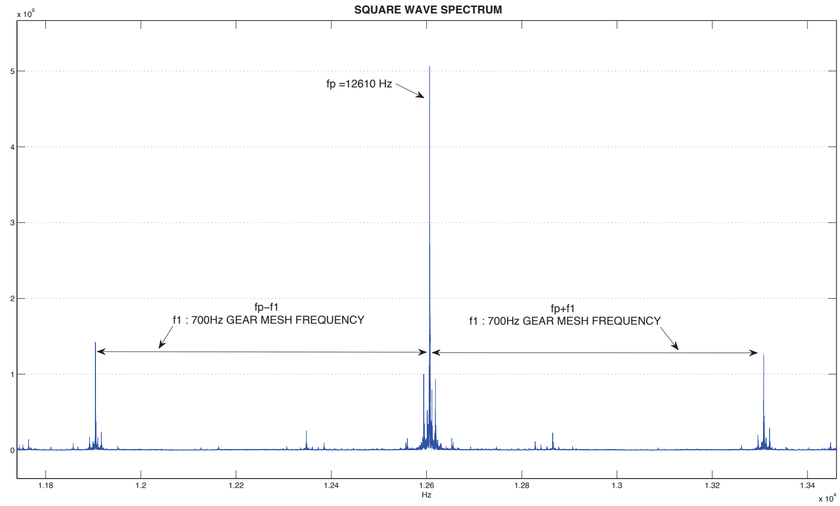

(b) Gear mesh frequency

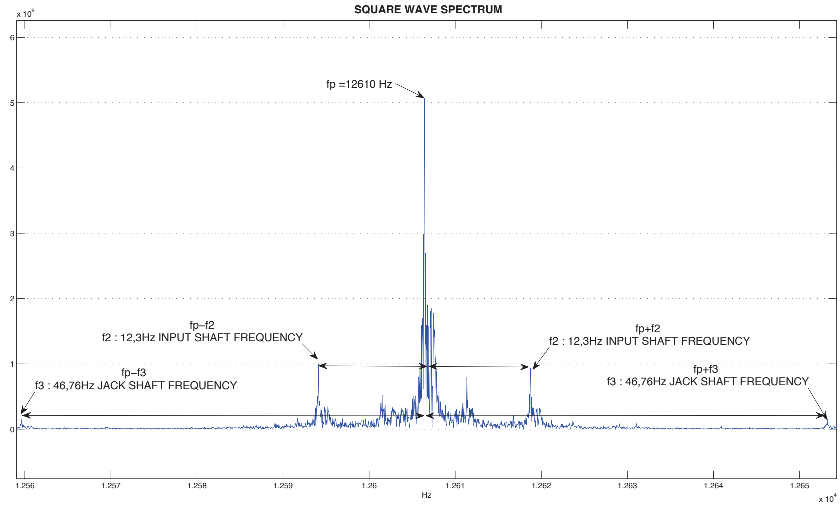

(c) shafts frequencies

Figure 2: Square wave spectrum

3 Twisted of a rotating shaft

3.1 Twisting of shaft

A shaft is twisted when the moment of all the forces act on a member about its polar axis, i.e. the moment normal to the section.The corresponding deformation is characterized by a twist angle θ .

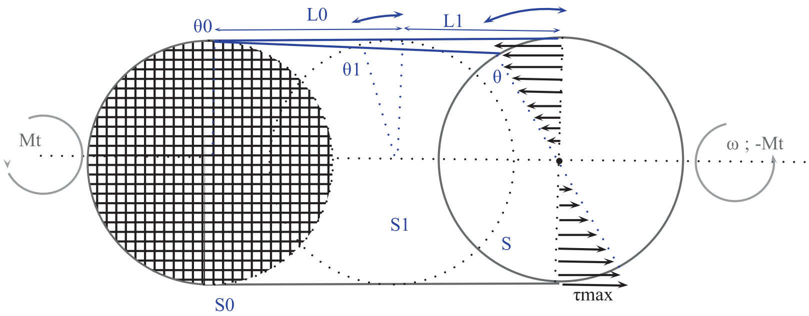

(a) Twisting of shaft

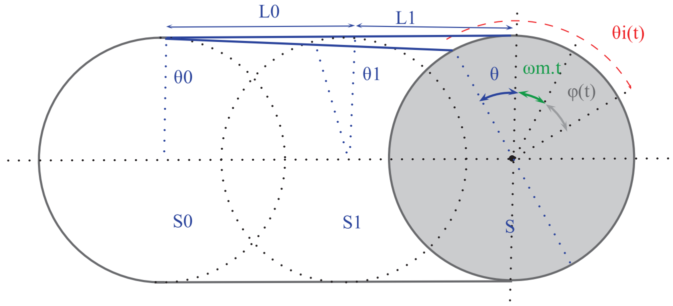

(b) Twisting combined with rotation

Figure 3: Shaft in twisting and in rotating

Assumption : The deal is a right circular cylinder of neglected weight. External forces are equivalent to two opposite couples which planes are perpendicular to the axis and coincide with the edge sections as showen in figure 3(a). We can consider that on one edge the cylinder is embedded and the other edge is subjected to a torque Mt. The maximal shear stress τ_{max} occurs at the point farthest from the cylinder axis. We note that :

- The twist angle is proportional to the distance of the free section

$$\frac{\theta_1 - \theta_0}{L_0} = \frac{\theta - \theta_1}{L_1} = \alpha, \tag{5}$$

- It is also proportional to the moment of torque Mt

$$Mt = \int\int_s G\alpha\rho^2 dS, \tag{6}$$

with :
- L_n the cylinder length (mm),
- θ_n the relating twist angle (rad) corresponding to the section S_n (mm^2),
- α the unit twist angle (rad/mm),
- G the Coulomb modulus (N/mm^2),

3.2 Twist combined with rotation

When the shaft is submitted to a twist and rotation, we can model its instantaneous phase as follows :

$$\theta_i(t) = \int \omega(t) = \omega_m t + \theta + \phi, \tag{7}$$

where :
- ω_m is the average speed (rad/s),
- θ is the twist angle, which depends on the mechanical stresses and on the material (rad),
- ϕ is the phase relating to fluctuations in shaft speed, which depends on the kinematic system (rad).

4 Estimation of the instantaneous phase $\theta_i(t)$: demodulation

We use "Hilbert Transform " HT to estimate the instantaneous phase of the square wave given by the optical encoder. The Hilbert transform decomposes a waveform into an instantaneous phase and an instantaneous amplitude waveform. If the signal shows an amplitude modulation, the instantaneous amplitude waveform would also show this modulation. Similarly, frequency modulation will affect the instantaneous phase waveform [Feldman, 2011].

A complex signal whose imaginary part is the HT of its real part is called an analytic or quadrature signal.

$$X(t) = x(t) + i\tilde{x}(t) \tag{8}$$

$$H[x(t)] = \tilde{x}(t) = \pi^{-1} \int_{-\infty}^{\infty} \frac{x(\tau)}{t-\tau} d\tau \tag{9}$$

Physically, the HT is an equivalent to a special kind of a linear filter, where all the amplitudes of the spectral components are left unchanged, but their phases are shifted by $-\frac{\pi}{2}$. Thus, if $x(t)$ is a real signal (please refer to the square wave given by the optical encoder figure 4(a)), It's the only one of the possible projections (the real part) of some analytic signal $X(t)$. The second projection of the same signal (the imaginary part) $\tilde{x}(t)$ will be conjugated according to the HT. A phasor can be viewed as a vector at the origin of the complex plane having a length $A_i(t)$ and an angular position (displacement) $\theta_i(t)$ such as

$$X(t) = |x(t)|[cos\theta_i(t) + isin\theta_i(t)] = A_i(t)e^{i\theta_i(t)}. \tag{10}$$

Using the trigonometric representation of the analytic signal, we can determine its instantaneous phase :

$$\theta(t) = arctan\frac{\tilde{x}(t)}{x(t)} = Im[LnX(t)], \tag{11}$$

and deduce the instantaneous frequency

$$f(t) = \frac{1}{2\pi}\frac{d\theta(t)}{dt}. \tag{12}$$

The HT may be implemented efficiently using the Fast Fourier Transform FFT [Bruns, 2004]. The first step is to treat the original signal with a bandpass filter around the fundamental frequency. The Fourier spectrum $S(\nu)$ of the original signal is multiplied by the transfer function $B_f(\nu)$, i.e. the bandpass filter in the frequency domain

$$S_f(\nu) = S(\nu).B_f(\nu). \tag{13}$$

The desired bandpass signal can be obtained by inverse FFT :

$$s_f(t) = TF_{\nu}^{-1}\{S_f(\nu)\}. \tag{14}$$

In the second step we calculate the Hilbert-Transformed bandpass spectrum :

$$H_f(\nu) = -isgn(\nu).S_f(\nu), \tag{15}$$

and its inverse FFT :

$$h_f(t) = TF_{\nu}^{-1}\{H_f(\nu)\}. \tag{16}$$

The bandpass signal $s_f(t)$ and its HT $h_f(t)$ finally constitute the real and the imaginary part, respectively, of the analytic signal

$$S^{HT}(f,t) = s_f(t) + ih_f(t). \tag{17}$$

Lastly we estimate the phase and the instantaneous frequency according to the formulas Eq(11) and Eq(12). Notice that, prior to the differentiation, we perform a unwrapping phase procedure to obtain a continuous phase. The unwrapping procedure produces a smooth increasing phase function by adding 2π every time a full cycle is completed. Right after the unwrapping phase we perform the differentiation according to Eq(12).

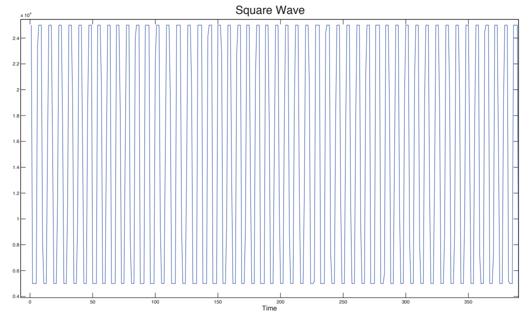

(a) Clipped square wave $x(t)$

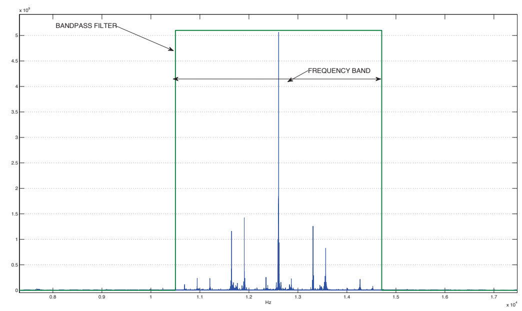

(b) Signal filtering $S_f(\nu)$

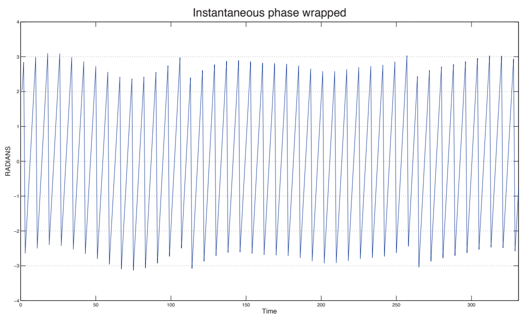

(c) Wrapped instantaneous angle $\theta_i(t)$

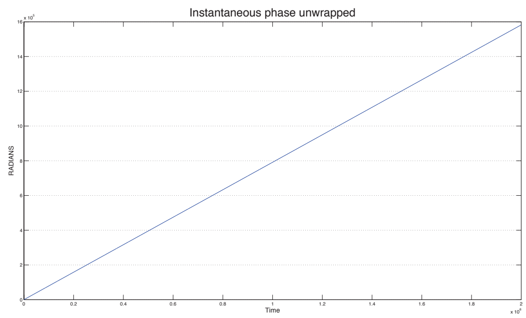

(d) unwrapped instantaneous angle $\theta_i(t)$

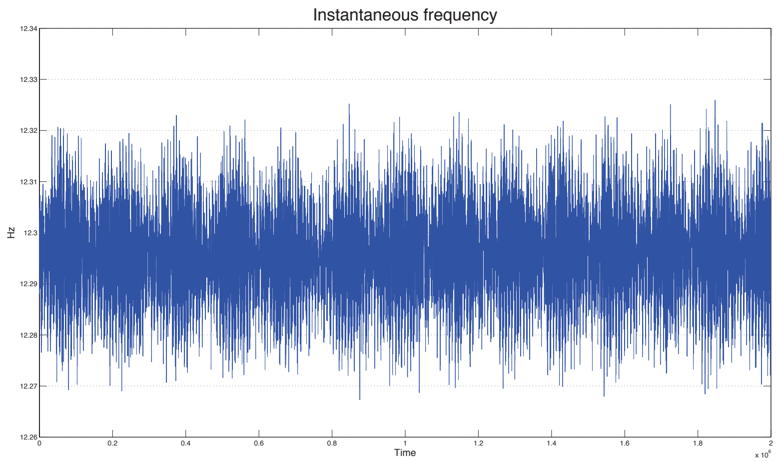

(e) Instantaneous frequency $f_i(t)$

Figure 4: Steps of Hilbert Tranform using FFT

5 Measure of the twist angle

We assume that the studied system shows no defects ($\phi \approx 0$) and that its operating parameters are unchanged (constant speed: 730 rev / min, constant resistant torque: 145 Nm). When we calculate the standard-deviation of the instantaneous phase $\theta_i(t)$, by considering the model proposed in Eq(7), we estimate the twist angle $\tilde{\theta}$ such as

$$\tilde{\theta}(t) = \sqrt{\frac{1}{N-1}\sum_{i=1}^{N}\Big(\theta_i(t) - \omega_m.t\Big)^2}. \tag{18}$$

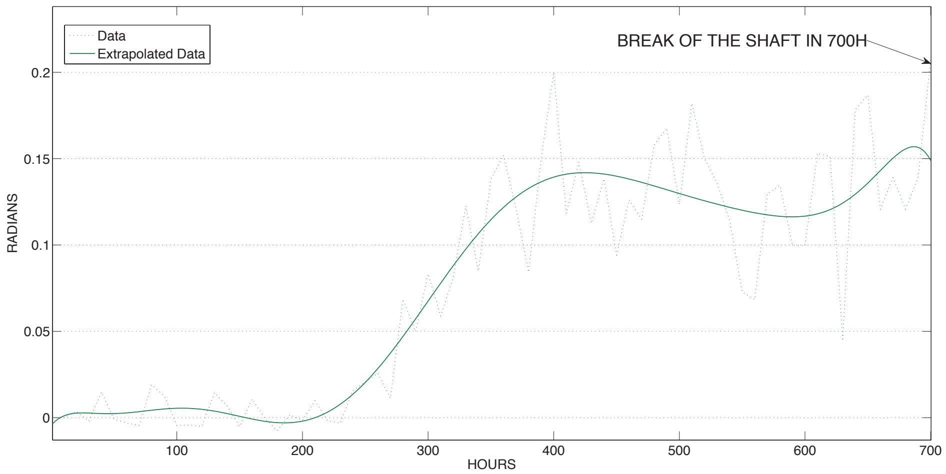

Figure 5: Standard-deviation of the instantaneous phase $\theta_i(t)$

The graph shows the standard-deviation trend of the instantaneous phase. In this graph, we can identify three parts:

- The first 200 hours. In this part, the shaft is rigid enough to resist twisting. The twist angle that we measure is zero.

- Between 200 hours and 450 hours. In this part, we assume that the shaft gets damaged as a result of fatigue and we observe a significant increase of the standard-deviation. This damage is manifested by a decrease in the rigidity of the shaft [D. Krajcinovic, 1987], and is characterized by an increase of twist angle. It seems that the increase is linear.

- The third part, between 450 and 700 hours. We assume that this is when the damage occurs. We observe a slight decrease and a sudden increase in the standard-deviation, leading to breakage.

6 Fatigue damage evaluation

The concept of damage was introduced by [Kachanov, 1958][Kachanov, 1994] in the context of isotropic damage by uniaxial creep. Kachanov and al. define the damage variable as a scalar D

$$0 \leq D \leq 1 \tag{19}$$

In the literature [Montheillet and Moussy, 1986], we have two groups of measurements techniques of damage. The first called **direct measurement**, which consists in observing the physical state of materials, and the second called **indirect measurement,** which principle is to measure physical parameters. The variation of Young's modulus E or of Coulomb's modulus G is one of this. Indeed, when a material gets damaged, the elastic constants, Young's modulus, Coulomb's modulus and Poisson's ratio decrease over time [D. Krajcinovic, 1987]. A mechanical analysis shows that these observations can be used to characterize the damage D by

$$D = 1 - \frac{\tilde{E}}{E}, \tag{20}$$

where E is the Young's modulus of the healthy state and $\tilde{E}$ is the Young's modulus when damage occurs. when $D = 0$ we are in a healthy state and when $D = 1$ we are in a damage state [Yu. N. Rabotnov, 1959]. So, knowing that $G = 0.4E$ [G. Buhot, 1967], we can write the equation

$$D = 1 - \frac{\tilde{G}}{G}. \tag{21}$$

If we consider the following assumptions on the shaft : The speed is constant , the geometry of the shaft does not change, the resisting torque is constant, and the rigidity of the shaft decreases during damage, equations Eq(6) and Eq(21) allow to express the damage scalar D as a function of the twist angle θ. We have then the relation

$$D(t) = 1 - \frac{\theta(t_0/t_f)}{\theta(t/t_f)}, \tag{22}$$

with
- $\theta(.)$ the twist angle,
- t_0 the initial time,
- t_f the time to failure.

So, we obtain the following.

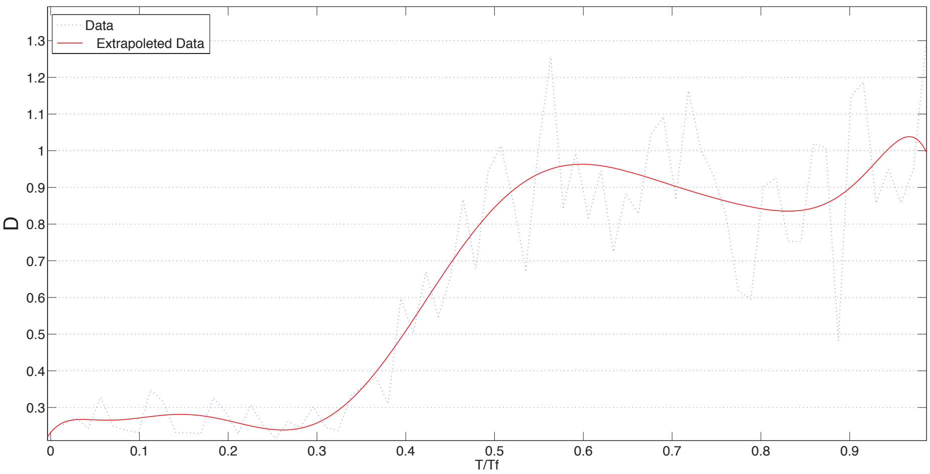

Figure 6: Damage evolution

This graph shows the damage percentage depending on the shaft lifetime. When the shaft is at 30% of its lifetime, it has less than 10% damage. From 30% of its lifetime the damage increases quickly and an 60% of its lifetime it's 90% damaged. The last 10% of damage occurs from 60% of its lifetime.

Currently a test bench of fatigue in torsion is implemented in order to reproduce this oberservation. The purpose is to use a lifetime law such as the Weibull distribution, to estimate the residual lifetime and compare it to the damage measure.

7 Conclusion

In this paper we propose a new indicator of fatigue damage : the standard-deviation of the instantaneous phase of a rotating shaft. Indeed, the instantaneous phase consists of a DC component and fluctuations related to the structure and to the kinematics of the system (ie defects). In the case studied, we found that the fatigue damage of the shaft increases in the same way as the standard-deviation until breakage. So we propose a model from which, according to some hypotheses (constant load and speed, geometry unchanged and no defects), we match the standard-deviation of the instantaneous phase to the shaft twist angle. Thus, from the speed signal, we can follow the twist angle and quantify the shaft damage. This approach expands the prospects of the diagnosis of rotating machines using as the speed signal.
Finally, I am extremely grateful for the collaboration of the GIPSA-Laboratory and for the available data of test bench GOTIX.

References

[Bruns, 2004] Bruns, A. (2004). Fourier-, hilbert- and wavelet-based signal analysis: are they really different approaches? *Journal of Neuroscience Methods*, 137(2):321 – 332.

[D. Krajcinovic, 1987] D. Krajcinovic, J. L. L. (1987). Continuum damage mechanics : Théory and application. *Springer Verlag*, pages 37–89.

[D. Shim and Ribbens, 1996] D. Shim, J. Park, P. P. K. and Ribbens, W. (1996). Reducing automotive engine speed fluctuation at idle. *IEEE transaction on Control Systems Technology*, 4:404–410.

[Desbazeille et al., 2010] Desbazeille, M., Randall, R., Guillet, F., Badaoui, M. E., and Hoisnard, C. (2010). Model-based diagnosis of large diesel engines based on angular speed variations of the crankshaft. *Mechanical Systems and Signal Processing*, 24(5):1529 – 1541. Special Issue: Operational Modal Analysis.

[Feldman, 2011] Feldman, M. (2011). Hilbert transform in vibration analysis. *Mechanical Systems and Signal Processing*, 25(3):735 – 802.

[G. Buhot, 1967] G. Buhot, P. T. (1967). *Cours de mécanique, résistance des matériaux*, volume 2. Masson et Cie, masson et cie edition.

[Kachanov, 1958] Kachanov, L. (1958). Rupture time process creep conditions. *international Journal of Fractures*, 97:11–18.

[Kachanov, 1994] Kachanov, L. M. (1994). On the concep of damage in creep and in brittle-elastic range. *international Journal of DAMAGE MECHANICS*, 3:329–337.

[Kumar et al., 2007] Kumar, S., Roy, N., and Ganguli, R. (2007). Monitoring low cycle fatigue damage in turbine blade using vibration characteristics. *Mechanical Systems and Signal Processing*, 21(1):480 – 501.

[Montheillet and Moussy, 1986] Montheillet, F. and Moussy, F. (1986). *Physique et mécanique de l'endommagement*. Les Editions de Physique.

[Renaudin et al., 2010] Renaudin, L., Bonnardot, F., Musy, O., Doray, J., and Rémond, D. (2010). Natural roller bearing fault detection by angular measurement of true instantaneous angular speed. *Mechanical Systems and Signal Processing*, 24(7):1998 – 2011. Special Issue: ISMA 2010.

[SNR-Industry, 2003] SNR-Industry (2003). Analyses et préconisations pour optimiser la vie des roulements.

[Xiaohua Yang and Wang, 1997] Xiaohua Yang, Nian Lit, Z. J. and Wang, T. (1997). A continuous low fatigue damage model and its application in engineering materials. *Journal Fatigue*, Vol.19:687–692.

[Yu. N. Rabotnov, 1959] Yu. N. Rabotnov, F. A. Leckie, W. P. (1959). "a mechanism of long time failure" in creep problems in structural members. *Journal of Applied Mechanics*, 37(1):249.